

Power Grid Optimal Topology Control Considering Correlations of System Uncertainties

Mohannad Alhazmi , *Student Member, IEEE*, Payman Dehghanian , Shiyuan Wang , *Student Member, IEEE*, and Bhavesh Shinde , *Student Member, IEEE*

Abstract—This article presents a probabilistic formulation and solution technique for the application of dc optimal power flow-based network topology control through transmission line switching strategies. Efficient utilization of the point estimation method (PEM) is pursued to model the system uncertainties, i.e., the stochastic load profile and the intermittent renewable generation. In order to address the computational effectiveness of the suggested probabilistic methodology, the PEM formulation is harnessed by a scenario reduction approach to capture the correlations of the system uncertainties, thereby achieving a more robust and faster operation solution for day-ahead and real-time applications. The proposed approach is applied to a modified IEEE 118-bus test system, where it demonstrates its attractive performance under different test scenarios. To further verify the efficiency and scalability of the proposed algorithms on large-scale systems, the proposed analytics are applied to 200-bus synthetic grid of central Illinois. AC feasibility and transient stability checks are performed on both test systems and the results are extensively analyzed.

Index Terms—Correlation, network topology control, probabilistic, switching, uncertainty.

NOMENCLATURE

A. Sets

$n \in \Omega_B$	Set of system buses.
$g \in \Omega_G$	Set of system generating units.
$k \in \Omega_L$	Set of system transmission lines.
$z \in \Omega_Z$	Set of uncertain variables.

B. Variables and Functions

$f_X(\cdot)$	Probability density function of variable X .
\overline{GC}^t	Expected total system generation dispatch cost probabilistically realized at time t .
G_W	Output power of a wind turbine (in MW).
\overline{P}_{D_n}	Vector of demand (in MW) at load bus n .
$\overline{P}_{d_n}^t$	Expected active power of bus n at time t .

Manuscript received February 13, 2019; revised July 9, 2019; accepted August 5, 2019. Date of publication August 11, 2019; date of current version October 18, 2019. Paper 2019-PSEC-0217.R1, presented at the 2019 Industrial and Commercial Power Systems Conference, Calgary, AB, Canada, May 5–8, and approved for publication in the IEEE TRANSACTIONS ON INDUSTRY APPLICATIONS by the Power Systems Engineering Committee of the IEEE Industry Applications Society. (*Corresponding author: Payman Dehghanian.*)

The authors are with the Department of Electrical and Computer Engineering, The George Washington University, Washington, DC 20052 USA (e-mail: alhazmi@gwu.edu; payman@gwu.edu; shiyuan12225@gwu.edu; shindebhavesh@gwu.edu).

Color versions of one or more of the figures in this article are available online at <http://ieeexplore.ieee.org>.

Digital Object Identifier 10.1109/TIA.2019.2934706

$\overline{P}_{g_n}^t$	Expected power output of generator g at bus n at time t .
$P_{g,n}^{\text{Wind}}$	Wind generation output at bus n .
P_{knm}^t	Power flow through transmission line k (connecting bus n to m) at time t .
$P_{z,i}, \lambda_{z,i}$	Probability and skewness of concentration i for random variable k .
v	Wind speed (m/s).
X, Y	Vectors of random input and output variables.
α_k	Switch action for transmission line k (1: no switch; 0: switch).
θ_n	Voltage angle at bus n .
$x(\cdot), (\cdot)$	Concentrations of X .
σ_x, μ_x	Standard deviation and mean value of random variable x .
$J(\cdot)$	Joint probability distribution function of random variables.

C. Dual Variables

η	Lagrange multipliers for equality constraints.
π	Lagrange multipliers for inequality constraints.

D. Parameters

B_k	Susceptance of transmission link k .
c_{g_n}	Linear generation cost of generating units g at bus n .
$E(\cdot)$	Expected value.
K, K', K''	Parameters of wind turbines.
M_k	Big- M value corresponding to line k .
$P_{g_n}^{\min}, P_{g_n}^{\max}$	Minimum/maximum generation limit of generator g at bus n .
P_k^{\min}, P_k^{\max}	Minimum/maximum limit on the power flow of transmission line k .
P_r	Rated power of a wind turbine (in MW).
v_i, v_r, v_o	Cut-in, rated, and cut-out wind speed (m/s).
r	Number of PEM input random variables.
$w(\cdot), (\cdot)$	Weighting factor.
$\xi(\cdot), (\cdot)$	Location of concentrations.
$\theta_n^{\min}, \theta_n^{\max}$	Minimum/maximum voltage angle at bus n .
ψ, β	Shaping and scaling coefficients of the Weibull probability distribution.

I. INTRODUCTION

POWER system topology control or transmission line switching (TLS) has been recognized, in theory and

practice, as a viable solution in hour- and day-ahead operations of electric transmission power grids [1], [2]. Utilizing the network existing infrastructure during the grid normal operating conditions, TLS results in a notable operational cost reduction. TLS can also be approached as a corrective action for power grid reliability improvement during critical contingencies [3], mitigation of voltage violations [4] and line overloads [5], ensuring system security [6], congestion management [7], and load outage recovery [8], [9]. Continuous variations in the electricity demand and the inherent uncertainties in renewable energy resources, if not modeled and handled properly, may compromise the application and attractiveness of the TLS technology in real-world practices.

In the past few decades, an eminent number of contributions have been recorded on hypothetical foundations with deterministic models and formulations for TLS applications in modern power transmission systems, primarily to achieve higher economic benefits and financial gains [10]–[14]. AC formulation of the topology control optimization is introduced in [15]. Out-of-market corrections of the ac infeasible market solutions for day-ahead accommodation of TLS are investigated in [16] and [17]. Scalability concerns of topology control implementations in real-world power systems are addressed in [18] and [19]. The effect of deterministic TLS on various electricity market features, with and without taking into account the $N-1$ reliability criterion, was investigated in [20] and [21]. A probabilistic security analysis taking into account the socioeconomic cost of disruptions and economic benefits of topology control solutions is suggested in [22], where two types of security aspects were studied integrated with the topology control program: cascading failures due to overloaded lines and steady-state voltage instability. Heuristic optimization models to handle the computational complexities of the large-scale TLS optimization problem are proposed in [23] and [24]. In dealing with the system uncertainties in TLS formulations, refs. [25] and [26] study chance-constrained formulation for topology control deployment in power systems primarily to accommodate higher utilization of wind generation. Robust optimization, where only the worst case uncertainty scenario is taken into account resulting in the most conservative TLS solutions, is suggested in [27]. For applications to large-scale power grids in the presence of a significant number of system uncertainties (stochastic load and intermittent renewables), a manageable-size and tractable formulation based on robust optimization models may not be computationally feasible.

The proposed model in this article is intended to be applied in hour-ahead operation of the grid: utilizing the network built-in flexibility to achieve economic benefits. In this proposed model, the system operator would know what transmission lines need to be switched ON/OFF based on the present information of the correlated uncertainties in system load and generation portfolios to achieve a more favorable economic benefit. Decisions for TLS either are currently not frequently adopted in practice by the transmission operator or are made in an ad hoc manner through a manual operator intervention. The reasons are multiple: lack of systematic decision-making tools, lack of proper training, and a lack of the mindset that will trust that such rather complex and

critical decisions can be automated and systematically applied. For this practice to be frequently realized in everyday operation, attempts need to be made to further develop robust tools for the operator decision making taking into account practical implementation concerns when exposed to various uncertainties originated from renewables, loads, and other unpredictable grid disruptions. To the best of the authors' knowledge, there has been limited effort on modeling and incorporating the correlation of system uncertainties into the TLS optimization formulations. This article puts forward a unique perspective to the conventional deterministic TLS optimization formulations. This article 1) introduces a probabilistic topology control formulation that can capture major uncertainties in the grid and stochastically assimilate such probabilistic features in network topology control optimization and 2) implements a scenario reduction technique driven by the correlation of system uncertainties to make this stochastic optimization model computationally friendly and tractable. AC feasibility and stability checks are performed to ensure that the proposed optimization solutions are in compliance with the desired network voltage and reactive power requirements and to ensure that switching transmission lines ON/OFF does not engender the network stability performance following their implementation.

The rest of the article is organized as follows. Section II presents background information on the topology control formulations for economic benefits. Section III introduces the proposed probabilistic optimization problem and the solution technique with the corresponding mathematical formulations. Section IV presents the numerical case studies and simulation results, followed by the conclusions in Section V.

II. POWER SYSTEM TOPOLOGY CONTROL

A. Deterministic TLS Models and Formulations

Deterministic TLS (DTLS) formulations assume that renewable generations and loads are all known at a given time instant with accurate forecasts available [28]. The system uncertainties are neither modeled nor incorporated. Typical formulations are based on dc optimal power flow (DCOPF) in hour-ahead or day-ahead applications and result in system minimum-cost solutions with transmission lines switching statuses. DTLS optimization can also be modeled in an ac setting where the solutions are more accurate, while the computational burden is more extensive.

B. Probabilistic TLS Models and Formulations

Probabilistic analysis is becoming increasingly important since 1) deterministic analysis cannot fully disclose the state of the system and 2) many random distortions or uncertainties arise from the measurement errors, forecasting errors, etc. exist. Uncertainties driven by renewable portfolios and the load variability are modeled in the probabilistic TLS (PTLS) formulations. Such probabilistic DCOPF-based optimization models are developed to find the optimal hour-ahead solution for network topology and generation dispatch that result in significant economic savings. In such formulations, uncertainties should

be first modeled and characterized, and then embedded into the PTLs optimization models.

1) *Uncertainty Characterization of Renewables and Loads:* Probability density function (PDF) and historical data are employed in this article to model the uncertainties driven by the high penetration of wind generation and the variable behavior of loads in the system. However, other approaches such as time series, artificial neural network, and regression techniques can be used to serve the same goal [29], [30]. The hourly wind speed is modeled by a Weibull probability distribution with the PDF expressed in (1) [31]. The model captures the sequential characteristic of the wind velocity and its impact on the output power of wind turbines. The Weibull distribution is utilized to characterize the wind speed since it provides a close approximation of the probability laws of many natural phenomena. It has been used to represent wind speed distributions for some time [32], [33]. The spectrum of wind speed realistically depends on a geographical location. The average wind direction is usually not zero and wind turbine has certain fixed orientation, typically along the most frequent wind. The Weibull distribution has proven to present the best fit to the wind speed data. Also, Weibull parameters could be easily determined from the observed wind speed frequency summaries [32]–[37]. Here, the PDF parameters are statistically estimated using the historical wind speed data by applying the curve fitting methods and maximum likelihood estimations. The output power of the wind generator is probabilistically calculated as a function of wind speed, formulated in (2)

$$f_v(v) = \left(\frac{\psi}{\beta}\right) \left(\frac{v}{\beta}\right)^{\psi-1} e^{-\left(\frac{v}{\beta}\right)^\psi}, \quad 0 \leq v \leq \infty \quad (1)$$

$$G_w = \begin{cases} 0, & 0 \leq v \leq v_i, v > v_o \\ (K + K' \times v + K'' \times v^2) \times P_r, & v_i \leq v \leq v_r \\ P_r, & v_r \leq v \leq \infty \end{cases}. \quad (2)$$

The load in the system is also another source of uncertainty, driven by many spatiotemporal variables, e.g., time, season, weather condition, electricity price, etc. The load uncertainties are modeled in this article through a Gaussian probability distribution with the PDF in (3)

$$f_{P_D}(P_D) = \frac{1}{\sqrt{2\pi\sigma_{P_D}^2}} \exp\left[-\frac{(P_D - \mu_{P_D})^2}{2\sigma_{P_D}^2}\right]. \quad (3)$$

We need to emphasize that the characterization accuracy and the corresponding errors are related to the forecasting aspect, which falls beyond the focus of this article.

2) *PTLS Optimization Formulation:* Performing a DCOPF-based DTLs optimization for every combination of the generation, load, and network topology is not viable or computationally intensive. The effective application of the point estimate method (PEM) is pursued in this article to probabilistically model the TLS formulation. Over the other probabilistic techniques [38], PEM is selected due to 1) its high level of accuracy, 2) its acceptable computational requirements, and 3) its success record of being implemented in various disciplines. PEM helps in

effectively capturing the impact of uncertain input variables and the propagation of such uncertainties over the output parameters. The vectors of the input and output random variables are characterized through nonlinear functions presented in (4)–(6), respectively

$$\mathbf{X} = [P_{g,n}^{\text{Wind}}, P_{D,n}] \quad (4)$$

$$Y = h(\mathbf{X}) = h(x_1, x_2, \dots, x_n) \quad (5)$$

$$Y = [\eta, \pi, GC^t]. \quad (6)$$

The probabilistic formulation of the DCOPF-based topology control optimization, so-called PTLs, is proposed and presented in (7), subject to several system and security constraints in (8)–(13) [14]

$$\min GC^t = \sum_{g \in \Omega_G, n \in \Omega_B} c_{gn} \overline{P_{gn}^t} \quad (7)$$

$$p_{gn}^{\min} \leq \overline{P_{gn}^t} \leq P_{gn}^{\max} \quad \forall g \in \Omega_G \quad (8)$$

$$P_k^{\min} \cdot \alpha_k \leq P_{knm}^t \leq P_k^{\max} \cdot \alpha_k \quad \forall k \in \Omega_L \alpha_k \quad (9)$$

$$\sum_{g \in \Omega_G} \overline{P_{gn}^t} - \sum_{m \in \Omega_B} P_{knm}^t = \sum_{d \in \Omega_D} \overline{P_{dn}^t} \quad \forall n \in \Omega_B \quad (10)$$

$$B_k \cdot (\theta_n - \theta_m) - P_{knm}^t + (1 - \alpha_k) \cdot M_k \geq 0 \quad \forall k \in \Omega_L \quad (11)$$

$$B_k \cdot (\theta_n - \theta_m) - P_{knm}^t - (1 - \alpha_k) \cdot M_k \leq 0 \quad \forall k \in \Omega_L \quad (12)$$

$$\alpha_k \in \{0, 1\} \quad \forall k \in \Omega_L. \quad (13)$$

Constraint (8) limits the output power of generating unit g at node n to its physical capacities. The power flow across transmission line k is limited within the minimum and maximum line capacities in (9). Constraint (10) enforces the power balance at each node. Kirchhoff's laws are incorporated in (11) and (12). An integer variable is introduced in constraint (13) reflecting the status (ON/OFF) of transmission line k in the system. Parameter M_k is a large number, which is used to make the constraints nonbinding and relax the one related to the Kirchhoff's laws when a line is removed regardless of the difference in the bus phase angles [14]. M_k is selected by the user in the range of $|B_K(\theta^{\max} - \theta^{\min})|$. In order to limit the number of open lines, χ is introduced in (14)

$$\sum_k (1 - \alpha_k) \leq \chi, \quad k \in \Omega_L. \quad (14)$$

C. AC Feasibility and Stability Checks

Since the DCOPF always assumes flat voltage profile of 1 per unit for the generators, it does not consider the reactive power and voltage constraints and, as a consequence, the resulting solutions may or may not be ac feasible. AC feasibility, hence, needs to be assessed for each proposed switching option. For ac power flow, the original network data excluding the opened lines with the generation schedules and loading patterns suggested by the topology control optimization algorithm are used. If the ac power flow does not converge, different adjustments may be tried to aid

the convergence with the available reactive power sources, e.g., shunts, generator voltage set points, transformer tap settings, etc. If ac feasibility is achieved with all the adjustments satisfying the generator reactive power constraints, then the transient stability is performed using the output of the ac load flow as the initial conditions for the machines. If the ac power flow is not feasible even with all the reactive power resources at their maximum limits, then the solutions are concluded infeasible. In practice, usually the utilities do some adjustments to the dc solution for ac feasibility. Even after all the possible adjustments, if the ac solution is not feasible, then the DCOPT solution needs to be rethought.

On the transient stability check, one needs to note that topology control action through TLS is considered a large disturbance in the system. Transient stability simulations, if simulated for longer time, will help in tracking both the initial impact of switching and the oscillatory behavior after the switching is implemented. For the transient stability simulations, the generation schedules and loading patterns corresponding to the switching actions are taken as the initial condition. Solution to an optimization problem in a dc setting followed by an ac feasibility and transient stability check can ensure that the solutions are realistically viable in real-world power grid operation that can be safely implemented [8].

III. PROPOSED METHODOLOGY

Considering the probability distributions allocated to system uncertain variables, the PEM decomposes (5) into several sub-problems by taking into consideration only $2n + 1$ deterministic values for each uncertain variable located on the right and left sides of the mean value. As a result, the PTLs optimization (7)–(13) is simulated $2n + 1$ times for each given set of the uncertain variables, while the other variables are kept constant at their mean values. The $2n + 1$ values can be selected either symmetrically or asymmetrically around the mean value [38]. Eventually, the PTLs formulation will result in the PDFs for the system generation dispatch cost and the most repeated status of each transmission line over the studied probabilistic scenarios.

A. Point Estimation Method

Even though PEM is analytically accurate and has been successfully applied to many problems in different disciplines, there are several limitations that can constrain its application to large-scale problems. Three main limitations are as follows [39]: 1) for every selected point in the input vector of random variables, it is a must that the Taylor series of the Z function converge; 2) infinite terms that exist in the Taylor series and may not match the real data set in real-world applications; and 3) only the information regarding the input random variables is required to assess the locations and weighting factors that are independent from the function Z .

1) $2n + 1$ PEM Scheme: The derivations for the $2n + 1$ PEM scheme in dealing with a multivariate problem (with multiple random variables) are presented in the following steps [39]:

Step 1: Take the Riemann–Stieltjes integral for the joint distribution function $J(X)$, where X is a vector of $X = (x_1, x_2, x_3, \dots, x_n)$. Mathematically, all PEMs will approximate the integral through a weighted sum of several function values assessed at a few selected points of the input random variables X

$$E(Z^k) = \int_D F^k(X) dJ(X). \quad (15)$$

Step 2: Apply the Taylor series to expand the $Z = F(\mathbf{X})$ at the mean μ_t value of the vector \mathbf{X} , where each random variable of X is independent. One can, hence, get

$$Z = \sum_{m_1=0}^{\infty} \dots \sum_{m_n=0}^{\infty} \frac{(x_1 - \mu_1)^{m_1} \dots (x_n - \mu_n)^{m_n}}{m_1! \dots m_n!} \cdot \left(\frac{\partial^{(m_1 + \dots + m_n)} F}{\partial x_1^{m_1} \dots \partial x_n^{m_n}} \right) (\mu_1, \dots, \mu_n). \quad (16)$$

Step 3: μ_z can be written as in (17), if each value of X in (16) converges to $F(X)$

$$\begin{aligned} \mu_z &= E(F(X)) = \int_D F(x) dJ(x) \\ &= \sum_{m_1=0}^{\infty} \dots \sum_{m_n=0}^{\infty} \frac{\lambda_{1,m_1} \sigma_1^{m_1} \dots \lambda_{n,m_n} \sigma_n^{m_n}}{m_1! \dots m_n!} \cdot \left(\frac{\partial^{(m_1 + \dots + m_n)} F}{\partial x_1^{m_1} \dots \partial x_n^{m_n}} \right) (\mu_1, \dots, \mu_n). \end{aligned} \quad (17)$$

Step 4: Let $F(X)$ be $F(\mu_1, \dots, \mu_{t-1}, x, \mu_{t+1}, \dots, \mu_n)$. The only variable is then X_t , while the other parameters are constant. Applying the Taylor series again, one gets

$$h_t(x) = h_t(\mu_t) + \sum_{i=1}^{\infty} \frac{1}{i!} h_t^{(i)}(\mu_t) (x - \mu_t)^i. \quad (19)$$

Step 5: Set $\xi_{t,1}$ and $\xi_{t,2}$ as the values to be determined, and set $\xi_{t,3}$ to be zero. We then define

$$\begin{aligned} S &= \sum_{t=1}^n (w_{t,1} h_t(x_{t,1}) + w_{t,2} h_t(x_{t,2}) + w_{t,3} h_t(\mu_t)) \\ &= F(\mu_1, \mu_2, \dots, \mu_n) \sum_{t=1}^n w_{t,3} \\ &\quad + \sum_{i=1}^{\infty} \sum_{t=1}^n \frac{1}{i!} h_t^{(i)}(\mu_t) (w_{t,1} \xi_{t,1}^i + w_{t,2} \xi_{t,2}^i) \sigma_t^i. \end{aligned} \quad (20)$$

Step 6: Both series, S and μ_z , are formed in a similar format. Such a similarity makes it possible to approximate μ_z using S by matching the first few terms. Then, set the following:

$$\sum_{t=1}^n (w_{t,1} + w_{t,2} + w_{t,3}) = 1 \quad (22)$$

$$w_{t,1} \xi_{t,1}^i + w_{t,2} \xi_{t,2}^i = \lambda_{t,i}, \quad i = 1, 2, 3, 4, \quad t = 1, 2, \dots, n \quad (23)$$

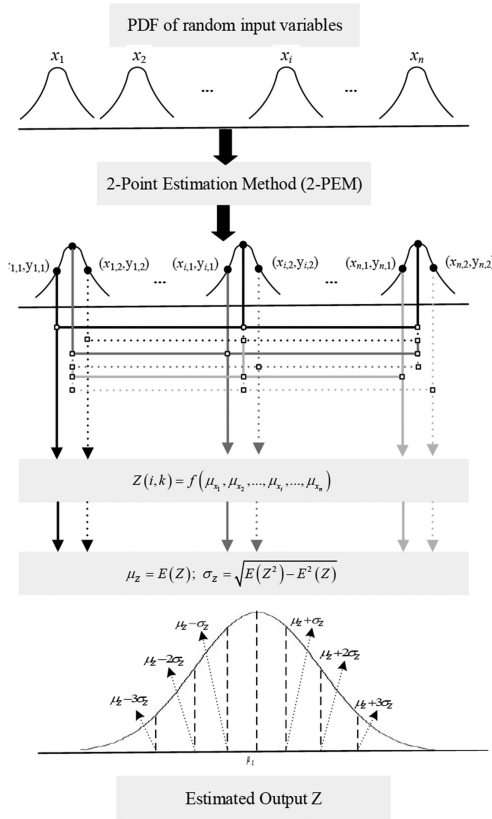


Fig. 1. Basic procedure of the PEM algorithm [41].

and assuming an equal probability for all variables X_t [40]

$$(w_{t,1} + w_{t,2} + w_{t,3}) = \frac{1}{n}, \quad t = 1, 2, \dots, n. \quad (24)$$

Step 7: Simultaneously solving (23) and (24) for random variable X_t ($t = 1, 2, 3, \dots, n$), the standard location and corresponding weighting factors are found as follows:

$$\xi_{t,k} = \begin{cases} \frac{\lambda_{t,3}}{2} + (-1)^{3-k} \sqrt{\lambda_{t,4} - \frac{3}{4}\lambda_{t,3}^2}, & k = 1, 2 \\ 0, & k = 3 \end{cases} \quad (25)$$

$$w_{t,k} = \begin{cases} (-1)^{3-k} \frac{1}{\xi_{t,k}(\xi_{t,1} - \xi_{t,2})}, & k = 1, 2 \\ \frac{1}{n} - \frac{1}{\lambda_{t,4} - \lambda_{t,3}^2}, & k = 3 \end{cases} \quad (26)$$

Further details on the aforementioned mathematical formulations can be found in [39] and [40].

2) *Two-Point Estimation Method:* In this article, the application of a two-point estimation method (2-PEM) is pursued, where n is selected to be two sample points of the input random variable, one located after and the other before its mean value. Fig. 1 illustrates the basic procedure in a 2-PEM algorithm. The following formulations are derived to implement the 2-PEM algorithm for probabilistic TLS optimization as follows [14], [38]: first, the requisite variables for the 2-PEM algorithm are initialized as presented in (27a) and (27b)

$$E(Y)^{(1)} = 0 \quad (27a)$$

$$E(Y^2)^{(1)} = 0. \quad (27b)$$

Then, the location and probability of concentrations are calculated through (28a)–(28d)

$$\xi_{z,1} = \frac{\lambda_{z,3}}{2} + \sqrt{r + \left(\frac{\lambda_{z,3}}{2}\right)^2} \quad \forall z \in \Omega_Z \quad (28a)$$

$$\xi_{z,2} = \frac{\lambda_{z,3}}{2} - \sqrt{r + \left(\frac{\lambda_{z,3}}{2}\right)^2} \quad \forall z \in \Omega_Z \quad (28b)$$

$$P_{z,1} = \frac{-\xi_{z,2}}{2r \cdot \sqrt{r + \left(\frac{\lambda_{z,3}}{2}\right)^2}} \quad \forall z \in \Omega_Z \quad (28c)$$

$$P_{z,2} = \frac{-\xi_{z,1}}{2r \cdot \sqrt{r + \left(\frac{\lambda_{z,3}}{2}\right)^2}} \quad \forall z \in \Omega_Z. \quad (28d)$$

One can then calculate the two concentrations $x_{z,1}$ and $x_{z,2}$ using the following equations:

$$x_{z,1} = \mu x, z + \xi_{z,1} \cdot \sigma x, z \quad (29a)$$

$$x_{z,2} = \mu x, z + \xi_{z,2} \cdot \sigma x, z. \quad (29b)$$

The next step is to run the deterministic TLS optimization with respect to the vector \mathbf{X} for concentrations $x_{z,1}$ and $x_{z,2}$

$$\mathbf{X} = [\mu_{z,1}, \mu_{z,2}, \dots, x_{z,i}, \dots, \mu_{z,r}], \quad i = 1, 2. \quad (30)$$

The following equations are then updated:

$$E(Y)^{(z+1)} \cong E(Y)^{(z)} + \sum_{i=1}^2 P_{z,i} \cdot h(\mathbf{X}) \quad (31a)$$

$$E(Y^2)^{(z+1)} \cong E(Y^2)^{(z)} + \sum_{i=1}^2 P_{z,i} \cdot h^2(\mathbf{X}). \quad (31b)$$

Finally, the expected value and the associated standard deviation of the output variables are found in (32)

$$\mu_Y = E(Y) \quad (32a)$$

$$\sigma_Y = \sqrt{E(Y^2) - E^2(Y)}. \quad (32b)$$

B. Correlation of Uncertainties and Scenario Reduction

If focusing on the conventional procedure in a $2n+1$ PEM (or 2-PEM), $2n+1$ (or 2) scenarios are generated for each random variable and the DTLs optimization problem should run for $2n+1$ (or 2) times concerning the random variable of interest. As the number of random input variables increases, the number of required DTLs simulation scenarios exponentially increases. All generated scenarios are assigned an equal realization probability of $1/\tau$. Considering the implementation requirements of the PTLs optimization in large-scale power grids with many random variables and in an operational time frame (hourly), a dimensionality reduction technique is needed to handle the sheer number of possible scenarios, making it computationally attractive.

A simple, yet efficient, scenario reduction technique is employed in this article. A two-dimensional matrix D , where $D \in R_+^{(N_R+1) \times \tau}$, is generated first, representing the random

TABLE I
12-H TIME-SERIES DATA OF UNCERTAIN WIND PATTERNS AND LOAD PROFILES

Time	P _w	P _d (1)	P _d (2)	Time	P _w	P _d (1)	P _d (2)
1	40	277	317	7	55	307	288
2	80	250	319	8	65	309	260
3	70	230	330	9	100	318	250
4	30	350	270	10	90	285	330
5	35	300	290	11	70	270	320
6	90	200	255	12	45	266	210

input variables, i.e., the intermittent generation and stochastic load profiles. The length of the data is considered equal to τ , and each row in matrix D represents a particular data set for the generation or load. The maximum and minimum values will be evaluated in each row of the matrix D , and all the other values between the maximum and minimum values are distributed into B_i number of bins, where $i \in [1, 2, 3, \dots, (N_R + 1)]$. The number of bins B is here arbitrarily selected and the axis of each bin is $(N_R + 1)$. Each bin is here representing one scenario, where the probability of each scenario is the number of counts inside the bin divided by the total number of the data points. The number of cells in each array is assigned a boundary of τ , reflecting the fact that at most τ cells are allocated values greater than zero [42].

An illustrative example is provided here to demonstrate the procedure of the scenario reduction technique. Table I presents 12-h time series corresponding to a 120-MW wind generator P_w and two loads— $P_d(1)$ and $P_d(2)$. The maximum and minimum values for the wind generation and the loads are [30–100], [200–350], and [211–330] MW, respectively. Each time series is normalized with respect to its corresponding maximum value. Three-dimensional bins (3×3) should be set up optionally, representing the three random input variables (load 1, load 2, and the wind generation), respectively. Each normalized value is distributed into the associated bin, and the number of observed values that fall in each bin is counted. Note that since the three-dimensional bins are in form of a $3 \times 3 \times 3$ array, the maximum number of possible scenarios is 27 [42].

Fig. 2 illustrates the counted number of data points in each bin. The middle cell in load 1 direction shows that the load 1 varies between 70% and 90% and load 2 changes between 0% and 70% of their maximum values, while the wind generation is 40–70% of its capacity. Note that this observation occurs in one particular hour (in 12 h). The probability of each scenario is the value of each cell divided by the number of total hours (e.g., 1 by 12 for this cell).

IV. NUMERICAL CASE STUDIES

In this section, the proposed approach is implemented on a modified IEEE 118-bus test system. Also, to ensure the performance scalability of the proposed methodology in large-scale real-world systems, we also demonstrate its applicability on the 200-bus synthetic grid of central Illinois. The optimization problem in all cases is run in General Algebraic Modeling System environment, using a Dell PowerEdge R815 with 4 AMD Opteron 6174 processors (48 2.2-GHz cores) and 256 GB of memory running CentOS 5.7. The PowerWorld Simulator is

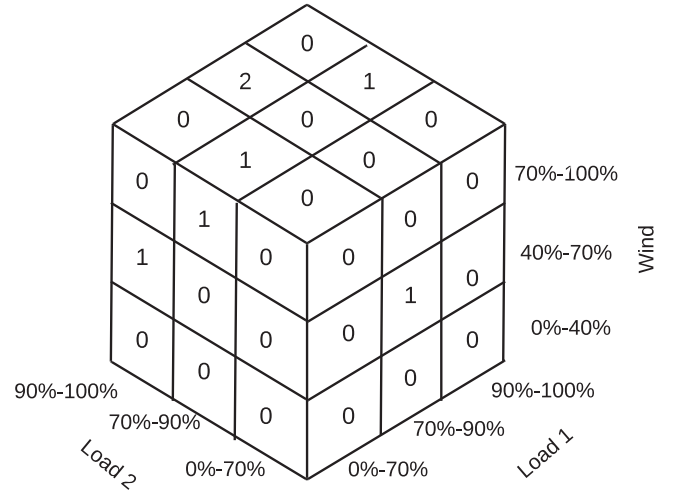


Fig. 2. Generated three-dimensional bins for scenario reduction.

TABLE II
SIMULATION RESULTS IN DIFFERENT STUDIED TEST CASES

Case #	Operation Cost (\$)	Time (sec.)	Switching Line
TC1	639.86894	0.02	Not Allowed
TC2	632.682627	0.02	14
TC3	629.596978	3.1	14
TC4	635.4567	0.052	14

used to perform the ac feasibility and stability checks and for performance visualizations.

A. Modified IEEE 118-Bus Test System

1) *System Descriptions, Data, and Assumptions:* The proposed approach is implemented on the IEEE 118-bus test system that consists of 185 transmission lines and 19 generating units (see Fig. 3) with 6859.2 MW installed capacity and a peak demand of 6000 MW. All system data (i.e., the hourly generation and load profiles, historical wind data, transmission line parameters, etc.) are provided in [43].

2) *Results and Discussions:* In order to demonstrate the performance of the suggested PTLs optimization and the solution technique, four different test cases (TCs) are studied: TC1 is the base-case study in which a deterministic OPF is performed with no topology control action allowed. TC2 and TC3 (presented in Section II) represent the cases in which DTLS (with known and accurate forecasts available, thereby solving a deterministic optimization) and PTLs (uncertainties are modeled) are performed, respectively. In TC3, 101 input random variables (2 wind generating units and 99 loads) are considered, resulting in 202 scenarios probabilistically handled via the 2-PEM. In TC4, the scenario reduction technique is applied to the PTLs optimization.

Simulation results, in terms of the system operation cost, the switching solutions, and the computational times in different test cases, are presented in Table II. Comparing the results in TC2 and TC3 with the base-case TC1, one can easily observe the economic advantages of harnessing the network built-in

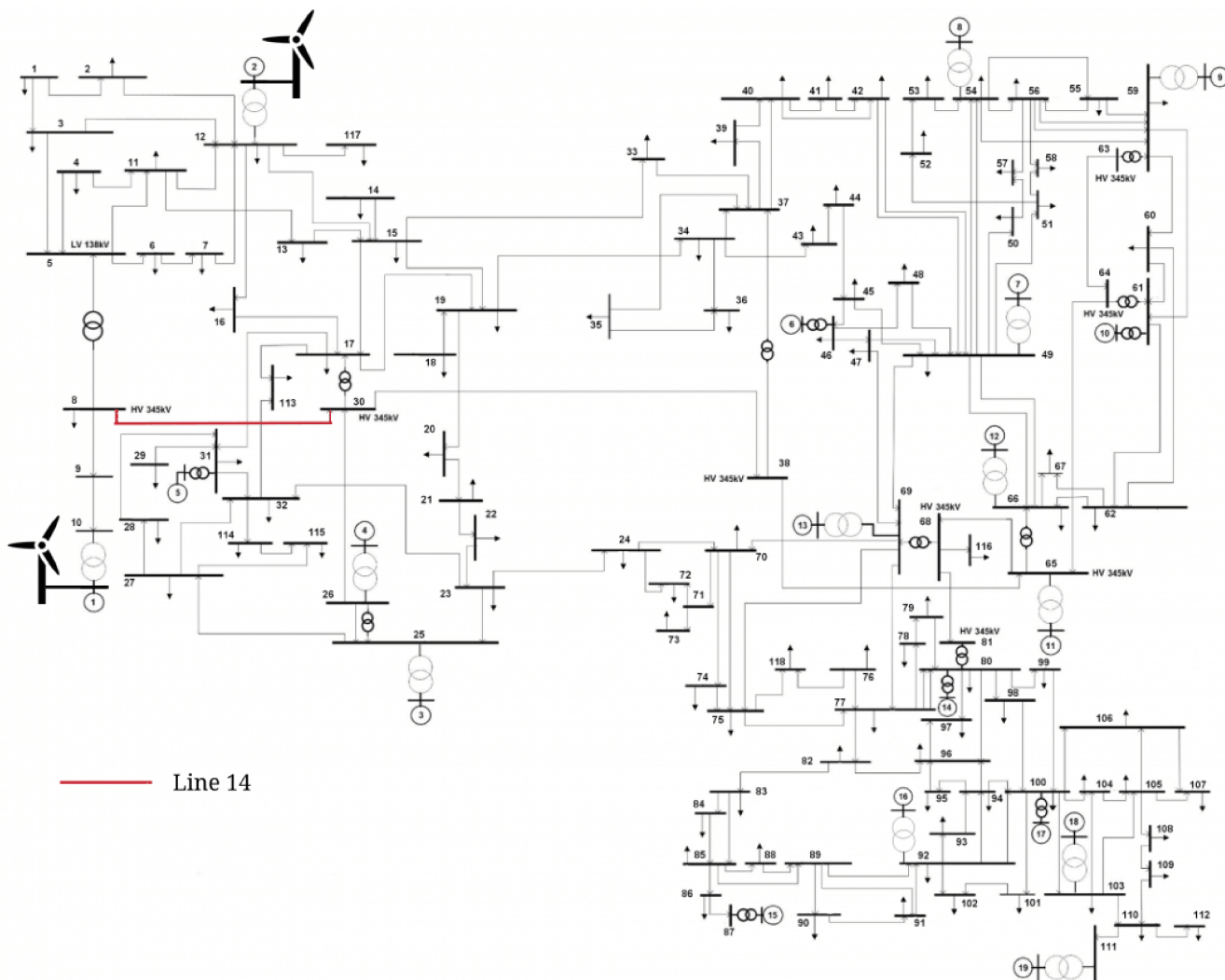


Fig. 3. IEEE 118-bus test system configuration.

TABLE III
CONCENTRATION FOR EACH BIN

Generation	90%- 93%	0	2	0
	93%- 96%	99	202	99
	96%- 100%	0	2	0
		90%- 93%	93%- 96%	96%- 100%
		Load		

TABLE IV
OPERATION COST AND COMPUTATION TIME IN EACH SCENARIO

Scenario #	Operation Cost (\$)	Time (sec.)
S1	637.025525	0.01
S2	601.786825	0.02
S3	633.301306	0.001
S4	673.636879	0.001
S5	628.335681	0.02

flexibility and topology control. TC2 will result in a total system cost of \$632.682, with transmission line 14 switched open. The computation time for TC2 is reported to be 0.02 s. The objective function and the computation time in TC3 are found to be \$629.596978 and 3.1 s, respectively. In TC4, where the correlations of the system uncertainties are managed through a scenario reduction technique, a reduced number of five scenarios are obtained. The PTLs optimization runs only five times, as opposed to TC3 with 202 simulations. Table III shows the concentrations found in each studied scenario. The total system operation cost in TC4 is found to be \$635.4567 and Table IV

summarizes the cost and simulation run-time in each scenario. Eventually, the dispatch solutions of the generating units in each studied test case are demonstrated in Fig. 6.

PowerWorld Simulator is used to check the grid performance following the solution implementation. Heat maps are generated that are based on the current flow ratings (in amperes) running through transmission lines. The current rating in the normal scenario is set from 0 to 460 A, where the maximum is set at 8016 A. Fig. 4(a) shows the system-wide line flow heat map when the TLS is not applied (TC1), reflecting the fact that the

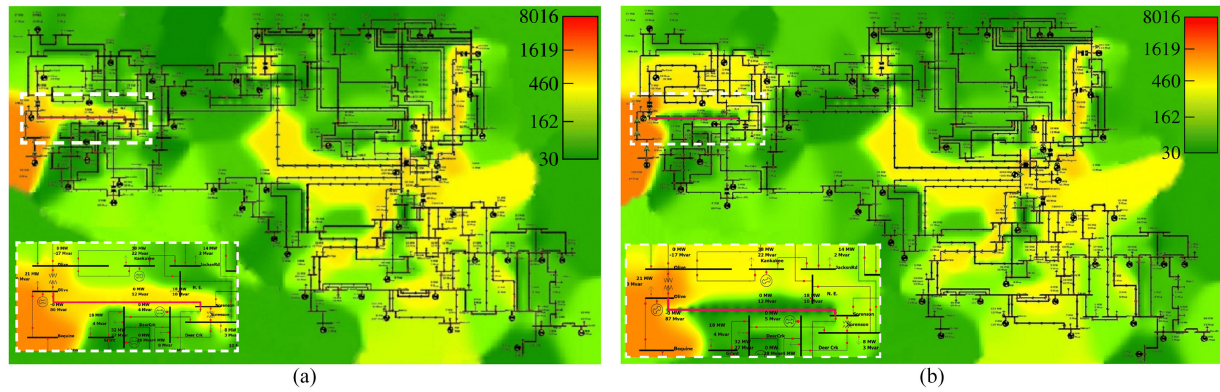


Fig. 4. Heat maps of the system current flows in the 118-bus test system. (a) TC1: base-case scenario. (b) TC3: TLS with correlated load and generation uncertainties.

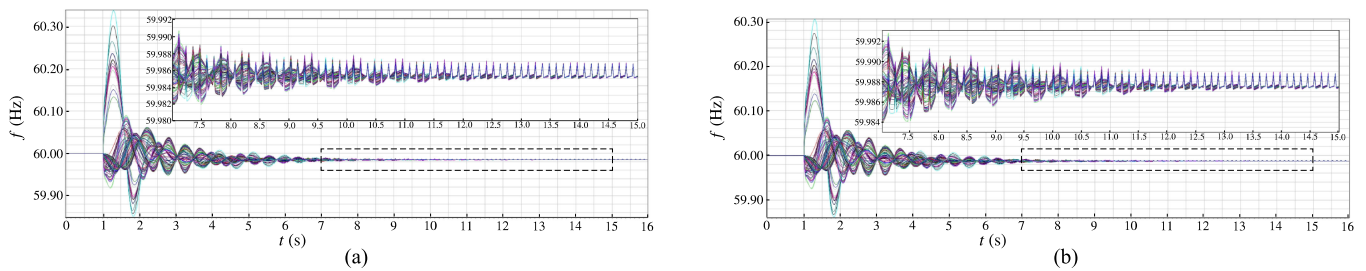


Fig. 5. Bus frequency results in the 118-bus test system. (a) TC2: TLS-only scenario. (b) TC3: TLS with correlated load and generation uncertainties.

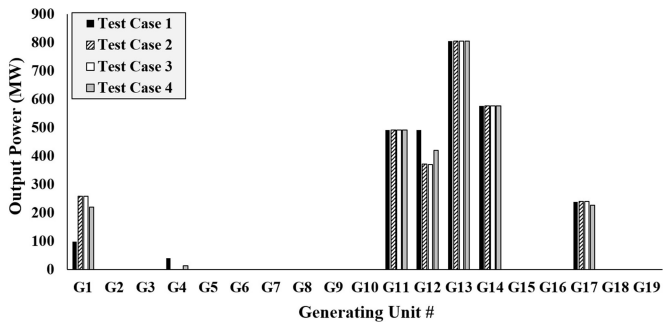


Fig. 6. Generation dispatch in different studied test cases.

power flows across the system are majorly within the desirable limits. Fig. 4(b) shows the system performance in TC3. The ac feasibility check is conducted confirming that the solution is ac feasible with all the AC optimal power flow (ACOPF) constraints satisfied. Transient stability analysis is performed for 16 s and the bus frequencies in TC2 and TC3 are demonstrated in Fig. 5(a) and (b), respectively. When transmission line 14 (connecting bus 8 to bus 30) is opened at both ends, the bus frequency graph shows a stable straight line at 60 Hz frequency until 1-s mark, after which a distortion appears in the graph where different generator bus frequencies vary ranging from 59.99 to 60.004 Hz until a certain point when all the generator buses converge to a stable state between 10.5 and 11.5 s on the graph, reflecting that the solution is stable.

TABLE V
SIMULATION RESULTS IN DIFFERENT STUDIED TEST CASES

Case #	Operation Cost (\$)	Time (sec.)	Switching Line
TC1	26397.681	0.01	Not Allowed
TC2	26395.681	0.19	160
TC3	26396.39122	6.64	160
TC4	25717.27254	0.1	160

B. Illinois 200-Bus System

1) *System Descriptions, Data, and Assumptions:* The proposed approach is tested on the 200-bus synthetic power grid of central Illinois. This case study is based on the real power system data and analysis [44]. This 200-bus system consists of 246 transmission lines and 40 generating units with 109.87174 MW peak demand and 3602.84 MW installed capacity. Data (i.e., the hourly generation and load profiles, historical wind data, transmission line parameters, etc.) are provided in [45].

2) *Results and Discussions:* The four TCs introduced earlier are also applied on this test system, the results on which are shown in Table V. The table presents the system operation cost, switching solutions, and the computational time in each test case. The operational cost and computational time in TC1 are found to be \$26 397.681 and 0.01 s, respectively. TC2 results in a system cost of \$26 395.681 and the computational time of 0.19 s with transmission line 160 switched open. In TC3, where the system uncertainties are modeled within 332 scenarios, the objective function and computation time are found to be \$26 396.39122

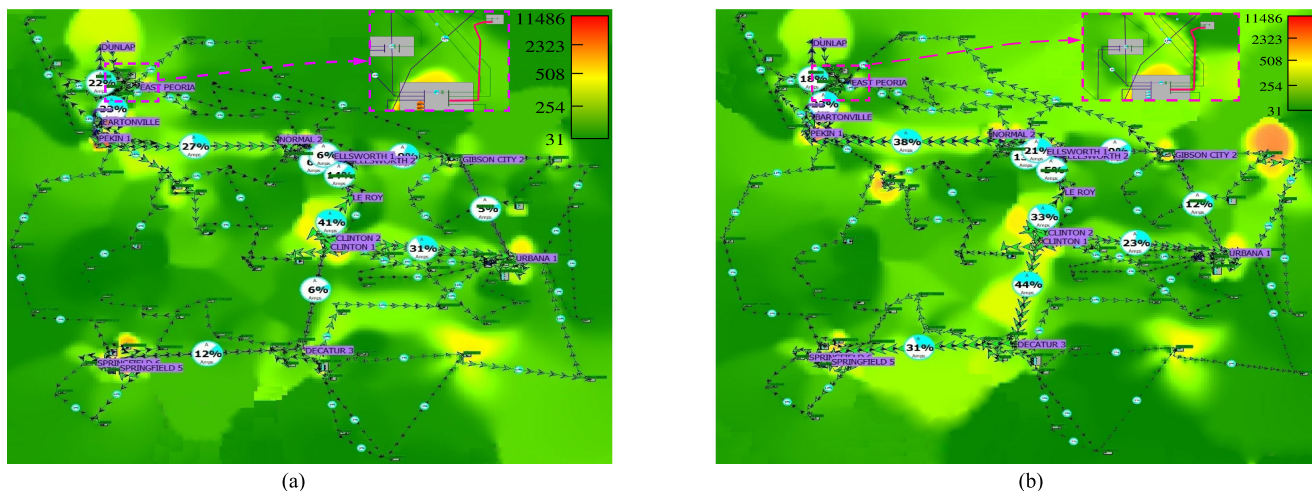


Fig. 7. Heat maps of the system current flows in 200-bus synthetic power grid of central Illinois. (a) TC1: base-case scenario. (b) TC3: TLS with correlated load and generation uncertainties.

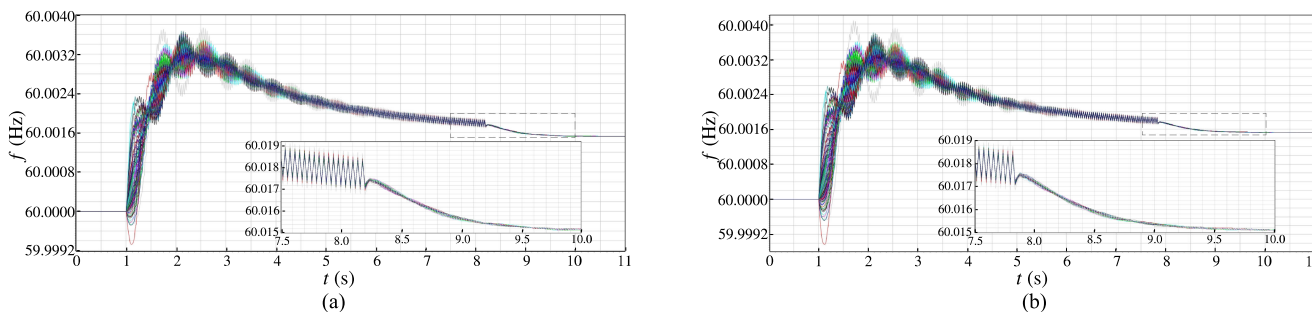


Fig. 8. Bus frequency results in the 200-bus test system of central Illinois. (a) TC2: TLS-only scenario text. (b) TC3: TLS with correlated load and generation uncertainties.

TABLE VI
OPERATION COST AND COMPUTATION TIME IN EACH SCENARIO

Scenario #	Operation Cost (\$)	Switching Line	Time (sec.)
S1	25702.075	160	0.02
S2	25096.436	160	0.02
S3	25671.2	160	0.02
S4	26437.551	160	0.02
S5	25630.033	160	0.02

TABLE VII
CONCENTRATION FOR EACH BIN

Generation	Load		
	90%- 93%	93%- 96%	96%- 100%
90%- 93%	0	6	0
93%- 96%	160	332	160
96%- 100%	0	6	0

and 6.64 s, respectively. Scenario reduction technique is applied in TC4, which results in a total system operation cost of \$25 717.27254 and computation time of 0.1 s. The economic advantage can be seen when comparing the base case condition (TC1) with other test cases. Additionally, comparison of the PTLs in TC3 and TC4 shows that the computation time is exponentially decreased in TC4, as the PTLs optimization runs only for five scenarios, contrasted to TC3 with 332 simulations.

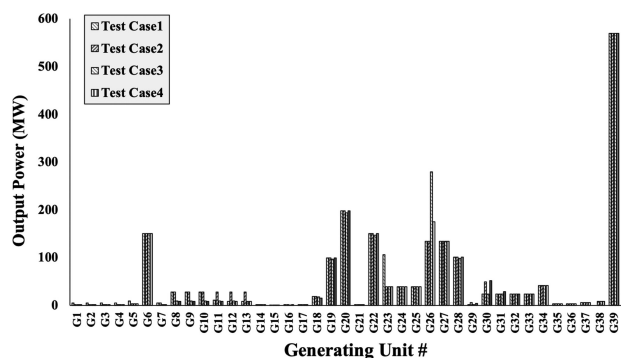


Fig. 9. Generation dispatch in different studied test cases.

Table VI presents the operational cost, computational times, and the switching solutions in each scenario in TC4. The concentration for each of the five scenarios is shown in Table VII. Furthermore, generation dispatch solutions for each TC are shown in Fig. 9.

To further study the practical considerations, PowerWorld Simulator is used to generate the heat maps on the system performance requirements. Heat maps are based on the current profile ratings in amperes running through the transmission

lines. The normal current rating is set from 0 to 508 A, where the maximum is set at 11 486 A. Fig. 7(a) shows the system heat map in TC1 and Fig. 7(b) shows the system performance in TC3 where the system correlated uncertainties are incorporated in the TLS optimization. The solution (switching out transmission line 160) passes the ac feasibility and transient stability checks, reflecting that the solution is safe to be implemented. The bus frequency results from the transient stability analysis of the system are demonstrated for TC2 and TC3, as shown in Fig. 8(a) and (b), respectively.

V. CONCLUSION

This article presented a probabilistic DCOPF-based formulation for the hour-ahead optimal topology control in power systems considering the correlations of stochastic variables. This probabilistic approach conjoins the PEM and a scenario reduction technique to statistically model and incorporate the system uncertainties (wind generation and load). AC feasibility and transient stability checks are performed to ensure a TLS solution is practically viable. Simulation results on the modified IEEE 118-bus test system demonstrated that the proposed probabilistic topology control framework with a scenario reduction technique can simultaneously improve the operation cost effectiveness and computational efficiency of the power grid operation optimization. The proposed approach is also tested on a large-scale test system, i.e., the 200-bus synthetic grid of central Illinois, and the results confirmed that the proposed methodology is scalable in real-world scenarios.

REFERENCES

- [1] M. Rezaeian Koochi, S. Esmaili, and P. Dehghanian, "Coherency detection and network partitioning supported by wide area measurement system," in *Proc. IEEE Texas Power Energy Conf.*, IEEE, 2018, pp. 1–6.
- [2] M. Rezaeian Koochi, P. Dehghanian, S. Esmaili, P. Dehghanian, and S. Wang, "A synchrophasor-based decision tree approach for identification of most coherent generating units," in *Proc. 44th Annu. Conf. IEEE Ind. Electron. Soc.*, IEEE, 2018, pp. 71–76.
- [3] H. Glavitsch, "Switching as means of control in the power system," *Int. J. Elect. Power Energy Syst.*, vol. 7, no. 2, pp. 92–100, 1985.
- [4] W. Shao and V. Vittal, "Corrective switching algorithm for relieving overloads and voltage violations," *IEEE Trans. Power Syst.*, vol. 20, no. 4, pp. 1877–1885, Nov. 2005.
- [5] A. A. Mazi, B. F. Wollenberg, and M. H. Hesse, "Corrective control of power system flows by line and bus-bar switching," *IEEE Trans. Power Syst.*, vol. PWRS-1, no. 3, pp. 258–264, Aug. 1986.
- [6] A. Khodaei and M. Shahidehpour, "Transmission switching in security-constrained unit commitment," *IEEE Trans. Power Syst.*, vol. 25, no. 4, pp. 1937–1945, Nov. 2010.
- [7] F. Kunz, "Congestion management in Germany: The impact of renewable generation on congestion management costs," pp. 1–18, 2011. [Online]. Available: http://idei.fr/sites/default/files/medias/doc/conf/eem/papers_2011/kunz.pdf
- [8] P. Dehghanian, Y. Wang, G. Gurralla, E. Moreno-Centeno, and M. Kezunovic, "Flexible implementation of power system corrective topology control," *Elect. Power Syst. Res.*, vol. 128, pp. 79–89, 2015.
- [9] P. Dehghanian, S. Aslan, and P. Dehghanian, "Maintaining electric system safety through an enhanced network resilience," *IEEE Trans. Ind. Appl.*, vol. 54, no. 5, pp. 4927–4937, Sep./Oct. 2018.
- [10] E. B. Fisher, R. P. O'Neill, and M. C. Ferris, "Optimal transmission switching," *IEEE Trans. Power Syst.*, vol. 23, no. 3, pp. 1346–1355, Aug. 2008.
- [11] M. Kezunovic, T. Popovic, G. Gurralla, P. Dehghanian, A. Esmailian, and M. Tasdighi, "Reliable implementation of robust adaptive topology control," in *Proc. 47th Hawaii Int. Conf. Syst. Sci.*, IEEE, 2014, pp. 2493–2502.
- [12] P. Dehghanian, T. Popovic, and M. Kezunovic, "Circuit breaker operational health assessment via condition monitoring data," in *Proc. North Am. Power Symp.*, IEEE, 2014, pp. 1–6.
- [13] P. Dehghanian and M. Kezunovic, "Impact assessment of transmission line switching on system reliability performance," in *Proc. 18th Int. Conf. Intell. Syst. Appl. Power Syst.*, IEEE, 2015, pp. 1–6.
- [14] P. Dehghanian and M. Kezunovic, "Probabilistic decision making for the bulk power system optimal topology control," *IEEE Trans. Smart Grid*, vol. 7, no. 4, pp. 2071–2081, Jul. 2016.
- [15] M. Soroush and J. D. Fuller, "Accuracies of optimal transmission switching heuristics based on DCOPF and ACOPF," *IEEE Trans. Power Syst.*, vol. 29, no. 2, pp. 924–932, Mar. 2014.
- [16] Y. Al-Abdullah, M. A. Khorsand, and K. W. Hedman, "Analyzing the impacts of out-of-market corrections," in *Proc. IREP Symp. Bulk Power Syst. Dyn. Control—IX Optim., Secur. Control Emerg. Power Grid*, IEEE, 2013, pp. 1–10.
- [17] Y. M. Al-Abdullah, M. Abdi-Khorsand, and K. W. Hedman, "The role of out-of-market corrections in day-ahead scheduling," *IEEE Trans. Power Syst.*, vol. 30, no. 4, pp. 1937–1946, Jul. 2015.
- [18] E. A. Goldis, X. Li, M. C. Caramanis, A. M. Rudkevich, and P. A. Ruiz, "AC-based topology control algorithms (TCA)—A PJM historical data case study," in *Proc. 48th Hawaii Int. Conf. Syst. Sci.*, IEEE, 2015, pp. 2516–2519.
- [19] X. Li, P. Balasubramanian, M. Abdi-Khorsand, A. S. Korad, and K. W. Hedman, "Effect of topology control on system reliability: TVA test case," in *Grid Future Symp.*, CIGRE US National Committee, pp. 1–8, 2014.
- [20] K. W. Hedman, M. C. Ferris, R. P. O'Neill, E. B. Fisher, and S. S. Oren, "Co-optimization of generation unit commitment and transmission switching with $n - 1$ reliability," *IEEE Trans. Power Syst.*, vol. 25, no. 2, pp. 1052–1063, May 2010.
- [21] R. P. O'Neill, R. Baldick, U. Helman, M. H. Rothkopf, and W. Stewart, "Dispatchable transmission in RTO markets," *IEEE Trans. Power Syst.*, vol. 20, no. 1, pp. 171–179, Feb. 2005.
- [22] P. Henneaux and D. S. Kirschen, "Probabilistic security analysis of optimal transmission switching," *IEEE Trans. Power Syst.*, vol. 31, no. 1, pp. 508–517, Jan. 2016.
- [23] P. A. Ruiz, J. M. Foster, A. Rudkevich, and M. C. Caramanis, "On fast transmission topology control heuristics," in *Proc. Power Energy Soc. Gen. Meeting*, IEEE, 2011, pp. 1–8.
- [24] J. D. Fuller, R. Ramasra, and A. Cha, "Fast heuristics for transmission-line switching," *IEEE Trans. Power Syst.*, vol. 27, no. 3, pp. 1377–1386, Aug. 2012.
- [25] F. Qiu and J. Wang, "Chance-constrained transmission switching with guaranteed wind power utilization," *IEEE Trans. Power Syst.*, vol. 30, no. 3, pp. 1270–1278, May 2015.
- [26] M. Nazemi, P. Dehghanian, and M. Lejeune, "A mixed-integer distributionally robust chance-constrained model for optimal topology control in power grids with uncertain renewables," in *Proc. 13th IEEE Power Energy Soc. PowerTech Conf.*, 2019, pp. 1–6.
- [27] A. S. Korad and K. W. Hedman, "Robust corrective topology control for system reliability," *IEEE Trans. Power Syst.*, vol. 28, no. 4, pp. 4042–4051, Nov. 2013.
- [28] M. H. Taheri, S. Dehghan, M. Heidarifar, and H. Ghasemi, "Adaptive robust optimal transmission switching considering the uncertainty of net nodal electricity demands," *IEEE Syst. J.*, vol. 11, no. 4, pp. 2872–2881, Dec. 2017.
- [29] J. Seguro and T. Lambert, "Modern estimation of the parameters of the Weibull wind speed distribution for wind energy analysis," *J. Wind Eng. Ind. Aerodyn.*, vol. 85, no. 1, pp. 75–84, 2000.
- [30] R. Billinton, H. Chen, and R. Ghajar, "A sequential simulation technique for adequacy evaluation of generating systems including wind energy," *IEEE Trans. Energy Convers.*, vol. 11, no. 4, pp. 728–734, Dec. 1996.
- [31] A. N. Celik, "A statistical analysis of wind power density based on the Weibull and Rayleigh models at the southern region of Turkey," *Renewable Energy*, vol. 29, no. 4, pp. 593–604, 2004.
- [32] E. K. Akpinar and S. Akpinar, "A statistical analysis of wind speed data used in installation of wind energy conversion systems," *Energy Convers. Manage.*, vol. 46, no. 4, pp. 515–532, 2005.

- [33] A. Azad, M. Alam, and M. R. Islam, "Statistical analysis of wind gust at coastal sites of Bangladesh," *Int. J. Energy Machinery*, vol. 3, no. 1, pp. 9–17, 2010.
- [34] E. C. Morgan, M. Lackner, R. M. Vogel, and L. G. Baise, "Probability distributions for offshore wind speeds," *Energy Convers. Manage.*, vol. 52, no. 1, pp. 15–26, 2011.
- [35] G. J. Herbert, S. Iniyen, E. Sreevalsan, and S. Rajapandian, "A review of wind energy technologies," *Renewable Sustain. Energy Rev.*, vol. 11, no. 6, pp. 1117–1145, 2007.
- [36] G. L. Johnson, *Wind Energy Systems*. Englewood Cliffs, NJ, USA: Prentice-Hall, 1985.
- [37] F. Odo, S. Offiah, and P. Ugwuoke, "Weibull distribution-based model for prediction of wind potential in Enugu, Nigeria," *Adv. Appl. Sci. Res.*, vol. 3, no. 2, pp. 1202–1208, 2012.
- [38] E. Rosenblueth, "Point estimates for probability moments," *Proc. Nat. Acad. Sci. USA*, vol. 72, no. 10, pp. 3812–3814, 1975.
- [39] Z. Lin and W. Li, "Restrictions of point estimate methods and remedy," *Rel. Eng. Syst. Saf.*, vol. 111, pp. 106–111, 2013.
- [40] H. Hong, "An efficient point estimate method for probabilistic analysis," *Rel. Eng. Syst. Saf.*, vol. 59, no. 3, pp. 261–267, 1998.
- [41] P. Dehghanian, "Power system topology control for enhanced resilience of smart electricity grids," Ph.D. dissertation, Dept. Elect. Comput. Eng., Texas A&M University, College Station, Texas, USA, 2017.
- [42] O. Ziaee, O. Alizadeh-Mousavi, and F. F. Choobineh, "Co-optimization of transmission expansion planning and TCSC placement considering the correlation between wind and demand scenarios," *IEEE Trans. Power Syst.*, vol. 33, no. 1, pp. 206–215, Jan. 2018.
- [43] "Data information." [Online]. Available: <https://www.flipsnack.com/mohannadalhazmi/data.html>. Accessed: Sep. 30, 2010.
- [44] A. B. Birchfield, T. Xu, K. M. Gegner, K. S. Shetye, and T. J. Overbye, "Grid structural characteristics as validation criteria for synthetic networks," *IEEE Trans. Power Syst.*, vol. 32, no. 4, pp. 3258–3265, Jul. 2017.
- [45] "Illinois 200-bus system: ACTIVSg200 data information." [Online]. Available: <https://electricgrids.engr.tamu.edu/electric-grid-test-cases/activsg200/>. Accessed: May 16, 2017.
- [46] M. Alhazmi, P. Dehghanian, S. Wang, and B. Shinde, "Power grid optimal topology control considering correlations of system uncertainties," in *Proc. IEEE/IAS 55th Ind. Commercial Power Syst. Tech. Conf.*, IEEE, 2019, pp. 1–7.



Mohannad Alhazmi received the B.Sc. and M.Sc. degrees in electrical engineering from Umm Al-Qura University, Mecca, Saudi Arabia, in 2013, and The George Washington University, Washington, DC, USA, in 2017, respectively. He is currently working toward the Ph.D. degree at the Department of Electrical and Computer Engineering, The George Washington University.

His research interests include power system control, reliability and resiliency, cybersecurity, and smart electricity grid applications.



Payman Dehghanian (S'11–M'17) received the B.Sc., M.Sc., and Ph.D. degrees in electrical engineering from the University of Tehran, Tehran, Iran, in 2009, the Sharif University of Technology, Tehran, Iran, in 2011, and Texas A&M University, College Station, TX, USA, in 2017, respectively.

He is currently an Assistant Professor with the Department of Electrical and Computer Engineering, The George Washington University, Washington, DC, USA. His research interests include power system protection and control, power system reliability and resiliency, asset management, and smart electricity grid applications.

Dr. Dehghanian was the recipient of the 2013 IEEE Iran Section Best M.Sc. Thesis Award in Electrical Engineering, the 2014 and 2015 IEEE Region 5 Outstanding Professional Achievement Awards, and the 2015 IEEE–HKN Outstanding Young Professional Award.



Shiyuan Wang received the B.Eng. degree in mechanical engineering from the University of Science and Technology Beijing, Beijing, China, in 2012, and the M.Sc. degree in electrical engineering from The George Washington University, Washington, DC, USA, in 2014. He is currently working toward the Ph.D. degree at the Department of Electrical and Computer Engineering, The George Washington University.

His research interests include power system reliability and resiliency, smart grid and renewable energy, power grid harmonic analysis, and application of signal processing in energy analytics.



Bhavesh Shinde received the B.Eng. degree in electrical engineering from Mumbai University, Mumbai, Maharashtra, India, in 2017. He is currently working toward the M.Sc. degree in electrical engineering at the Department of Electrical and Computer Engineering, The George Washington University, Washington, DC, USA.

His research interests include deep machine learning applications in power systems, cybersecurity, and power system resilience.